SPALL AND DYNAMIC YIELDING OF ALUMINUM AND ALUMINUM ALLOYS AT STRAIN RATES OF 3×10 6 s −1

D. A. Dalton, D. L. Worthington, P. A. Sherek, N. A. Pedrazas, A. C. Bernstein, H. J. Quevedo, P. Rambo, J. Schwarz, A. Edens, M. Geissel, I. C. Smith, E. M. Taleff, and T. Ditmire

Citation: AIP Conference Proceedings **1195**, 969 (2009); doi: 10.1063/1.3295307

View online: http://dx.doi.org/10.1063/1.3295307

View Table of Contents:

http://scitation.aip.org/content/aip/proceeding/aipcp/1195?ver=pdfcov

Published by the AIP Publishing

CP1195, *Shock Compression of Condensed Matter - 2009*,
edited by M. L. Elert, W. T. Buttler, M. D. Furnish, W. W. Anderson, and W. G. Proud

SPALL AND DYNAMIC YIELDING OF ALUMINUM AND ALUMINUM ALLOYS AT STRAIN RATES OF $3x10^6$ s^{-1}

D.A. Dalton[1], D.L. Worthington[2], P.A. Sherek[2], N.A. Pedrazas[2], A.C. Bernstein[1], H.J. Quevedo[1], P. Rambo[3], J. Schwarz[3], A.Edens[3], M. Geissel[3], I.C. Smith[3], E.M. Taleff[2], T. Ditmire[1]

[1]*Dept. of Physics, University of Texas at Austin, 1 University Station C1600, Austin, TX 78712*
[2]*Dept. of Mechanical Engineering, University of Texas at Austin, 1 University Station C2200, Austin, TX 78712*
[3]*Sandia National Laboratories, Z-Backlighter Facility, Albuquerque, NM 87185*

Abstract. We have explored the role that grain size, impurity particles and alloying in aluminum play in dynamic yielding and spall fracture at tensile strain rates of ~$3x10^6$ s^{-1}. We achieved these strain rates shocking the aluminum specimens via laser ablation using the Z-Beamlet Laser at Sandia National Laboratories. The high purity aluminum and 1100 series aluminum alloy produced very different spall strengths and nearly the same yield strengths. In contrast, various grain-sized Al + 3 wt. % Mg specimens presented the lowest spall strength, but the greatest dynamic yield strength. Fracture morphology results and particle analysis are presented along with hydrodynamic simulations to put these results in context. Impurity particles appeared to play a vital role in spall fracture at these fast strain rates. Alloying elements such as Mg seem to be the dominant factor in the dynamic yield results.

Keywords: Aluminum, VISAR, spall, fracture.
PACS: 42.79.Qx, 62.20.-x.

INTRODUCTION

Spall is the planar fracture of material at fast strain rates due to a tensile stress, such as that initiated by explosives, plate impacts, or pulsed laser irradiation. When an intense laser irradiates a solid target, an ablation-driven shock-wave propagates through the material, reflects off the rear (free) surface and produces a rarefaction wave back into the target. The material is put into tension as this rarefaction wave encounters the rarefaction from the decay of the still forward-going shock. When the resulting tensile stress surpasses the maximum tensile strength for the material under the given loading conditions, the material spalls.

Spall experiments on single crystal aluminum foils were performed to eliminate the effect of grain boundaries so we can measure the inherent strength of the crystalline material rather than the strength of grain cohesion. The single crystal materials of interest were high purity aluminum (Al-HP) and 1100 series aluminum (Al-1100). In addition to the single crystal specimens, we investigated Al + 3 wt. % Mg (Al+3Mg) at 3 different grain sizes.

EXPERIMENTAL PROCEDURE

To generate the shock we use the Z-Beamlet Laser (ZBL). ZBL is a 1.2 kJ laser of frequency-

doubled light at 527 nm and pulse length of 1.8 ns. The pulse shape was square and had a top-hat intensity profile. The laser was focused with an f/8 optic and the target was placed ~50 mm away from focus to achieve a spot size 5.8 mm wide.

The target thicknesses used in our experiments were 350 μm and 500 μm. The 350 μm targets were impacted at (9±2) x 10^{11} W/cm^2 and produced a tensile strain rate of ~3-4 x 10^6 s^{-1}. The 500 μm targets were impacted at (1.5±0.4) x 10^{12} W/cm^2 and produced a tensile strain rate of ~2-3x10^6 s^{-1}. For the 350 μm (500 μm) targets, the pressure near the rear surface was 66±13 kbar (64±8 kbar).

A line-VISAR diagnostic is used to measure the free surface velocity of the target specimens. Light reflecting from a moving surface produces Doppler shifted light which is interfered with itself at a later time to produce temporal interference where the fringe shifts are proportional to the free surface velocity. The VISAR diagnostic closely follows the design features of Celliers, et al. [1]. The line-VISAR probe beam is produced by a single-longitudinal mode laser (Spectra-Physics Lab-130 Laser, 532 nm, ~80 mJ, 8 ns FWHM) and a pulse stacker is used to stretch the pulse to 30 ns [2]. The spall strength (P_{spall}) and HEL stress (σ_{HEL}) were determined by:

$$P_{spall} = \frac{1}{2}\rho_0 \cdot c \cdot \Delta u , \qquad (1)$$

$$\sigma_{HEL} = \frac{\rho_0 U_e u_{fse}}{2} , \qquad (2)$$

where ρ_0 is the material density, c is bulk sound speed, Δu is pullback velocity, u_{fse} is the free surface velocity of the elastic precursor and U_e is approximated as the elastic wave speed.

The Al-HP is 99.999% high purity aluminum. The Al-1100 is 99% Al with moderate amounts of iron and silicon impurities. The Al+3Mg specimens have a large concentration of magnesium atoms and a fairly large amount of iron impurities. The average grain sizes of the Al+3Mg are 295 μm, 44 μm and 29 μm.

RESULTS

Al-HP and Al-1100 Results

Figure 1 shows an interferogram and a resulting velocity lineout. Table 1 summarizes the target thickness (t), average spall strength and average HEL stress for Al-HP and Al-1100.

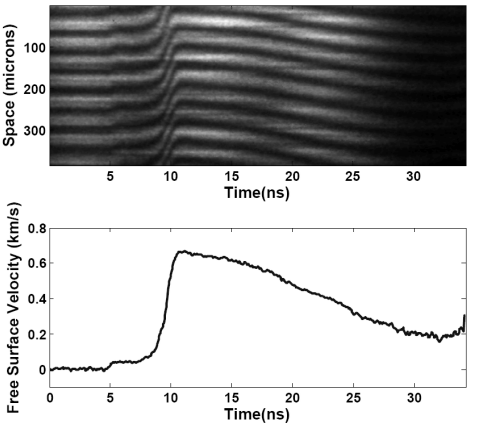

Figure 1. Interferogram and resulting velocity lineout for 510 μm Al-HP impacted at 9x10^{11} W/cm^2 resulting in a spall strength of 36 kbar and tensile strain rate of 3x10^6 s^{-1}. The HEL stress was determined to be 3.7 kbar.

The Al-HP exhibited a 20% higher spall strength than the Al-1100. We also observed that the Al-HP had a low dynamic yield stress. This is likely due to the absence of alloying elements, which allows dislocations to move freely.

Table 1. Single crystal specimens

Material	t (μm)	P_{sp} (kbar)	σ_{HEL} (kbar)
Al-HP	350	35	2
	500	35	2
Al-1100	350	29	1

Fracture analysis of the targets revealed various features. In the single crystal Al-HP, ductile dimples were evident. In the single crystal Al-1100, ductile dimples were also observed; however, at the center of these dimples were iron-rich impurity particles. This leads us to believe that in single crystal Al-1100, microvoid nucleation takes place at iron rich particles. In contrast,

microvoid nucleation within the single crystal Al-HP does not typically take place at grains or impurity particles. Ductile fracture results from the coalescence of microvoids and it is the mechanism of spallation failure in these materials. For the Al-1100, the ratio of average particle spacing to average dimple spacing is ~1, meaning that iron rich impurity particles are likely initiating fracture in this material. On the contrary for the Al-HP, the ratio of average particle spacing to average dimple spacing is >>1, meaning that impurity particles are not readily available to initiate fracture in materials at these strain rates. Comparison of the post shot fracture analysis and VISAR results leads us to conclude that iron rich particles in Al-1100 yields smaller spall strength; however, these particles do not contribute to any significant compressive yield strengthening.

HYADES simulations were used for comparison with experiments [3]. Figure 2 shows the velocity lineout for Al-HP for von-Mises and Steinberg-Guinan [4] yield models with a constant spall value of 33 kbar. Lower intensities are needed to meet the measured peak velocities.

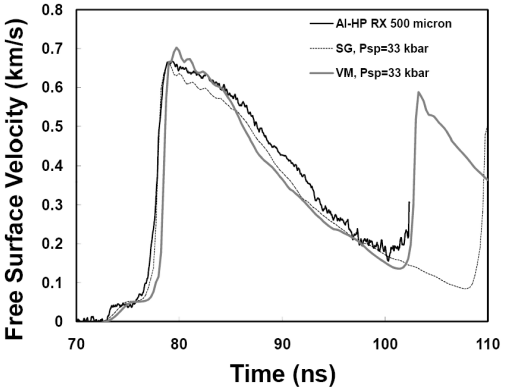

Figure 2. HYADES simulations showing free surface velocity versus time compared to data. SG and VM are Steinberg-Guinan and von-Mises yield models.

Al+3Mg Results

Table 2 shows a summary of the target specimen details and dynamic results for the Al+3Mg. While the spall strength and HEL stress results show no clear dependence with grain size, the surprising result is that there is an apparent dependence of fracture mode on grain size.

Two distinct fracture modes were observed in the Al+3Mg. In the large grained material (295 μm), or quasi-single crystal material, the fracture was predominantly transgranular and ductile in nature. For the small grained material, the fracture was mostly brittle intergranular but with some areas of ductile dimpling. Iron-rich particles are also present at the pits of the ductile dimples.

Table 2. Al+3Mg specimens

Material	t (μm)	Grain Size (μm)	P_{sp} (kbar)	σ_{HEL} (kbar)
Al+3Mg	350	295	26	15
	350	44	26	18
	350	29	25	16

We postulate that in fine grained polycrystalline materials the nucleation sites for spall are initiated at grain boundaries which are the longer length scale imperfections. Secondly, ductile fracture is initiated in the grains at particles which are micrometer scale imperfections. In the quasi-single crystal (coarse-grained) Al+3Mg, the nucleation sites for spall are at secondary particles.

DISCUSSION

At strain rates of 10^6 to 10^7 s^{-1}, spall fracture is determined by imperfections in the material. The length scales of the imperfections are vital to the type of fracture and to the maximum stress that can be supported in these materials.

The HEL stresses found in these shots were not well defined, meaning the free surface velocities did not come to a sharp peak, decay and then increase again. This is consistent with what G.I. Kanel found previously [5]. The authors also determined that when heated to higher temperatures, the HEL stress does become better defined. This is due to the phonon drag mechanism being increased at higher temperatures.

With respect to single crystal orientation, Chen, et al. reported that single crystal [100] Al had the highest spall strength and that it consistently had 40% higher spall strength than polycrystalline aluminum [6]. The authors also observed an

increase in pullback velocity with impact stress. They also saw that pullback signals for polycrystalline Al differs by a large amount at 40 kbar but were similar at 220 kbar.

In general we observed that the Al+3Mg had the highest dynamic yield stress and showed no dependence with grain size. This is likely due to the magnesium atoms within the matrix of aluminum. The size of the magnesium atoms compared to the aluminum atoms likely yielded a stress field which inhibits dislocations from moving through the grains, i.e. solid-solution strengthening. We did not observe any trend with grain size, which is surprising, considering that smaller grains should inhibit the movement of dislocations. One must keep in mind that yield strengthening due to the grain size effect does not greatly affect aluminum compared to other metals like copper, even at engineering strain rates.

In contrast to the Al+3Mg data, we saw that the Al-HP RX had a much lower dynamic yield stress. This is likely due to the absence of alloying elements, which allows dislocations to move freely. The Al-1100 showed very little evidence of an elastic precursor and in some cases exhibited no precursor at all. The absence of a precursor in some cases may be due to a slightly higher energy shot.

CONCLUSIONS

First, single crystal Al-HP exhibited the highest spall strength (35 kbar), whereas single crystal Al-1100 exhibited the second highest spall strength (29 kbar). The fracture of the Al-HP was limited by the strength of the crystal, while fracture of the Al-1100 was initiated by iron rich particles.

Secondly, the Al+3Mg specimens presented the smallest spall strength (26 kbar). There was no obvious trend in the spall strength data among the different grain sizes of Al+3Mg. The fracture of Al+3Mg was initiated by both impurity particles and grain boundaries.

Finally, single crystal Al-HP and Al-1100 produced a relatively low HEL stress compared to the Al+3Mg. The Al+3Mg yield strength was likely increased by the presence of magnesium atoms. The Al-HP and Al-1100 had no such strengthening center.

ACKNOWLEDGEMENTS

This work was supported by the Army Research Office and National Nuclear Security Administration. Support of the National Science Foundation under grant DMR-0605731 is gratefully acknowledged.

REFERENCES

1. Celliers, P.M. et al., "Line-imaging velocimeter for shock diagnostics at the OMEGA laser facility", Review of Scientific Instruments **75,** 4916, 2004.
2. Dalton, D.A. et al., " A non-interferometric pulse-stacker for diagnostic and energetic laser applications" in Conference on Lasers and Electro-Optics 2008, San Jose, CA 2008.
3. Larsen, J.T., Lane, S.M.., "HYADES- a plasma hydrodynamics code for dense plasma studies", **51**, 179, 1994.
4. Steinberg, D.J., Cochran, S.G., Guinan, M.W., "A constitutive model for metals applicable at high strain rates" Journal of Applied Physics **51,** 1498, 1980.
5. Kanel, G.I., Razorenov, S.V., Baumung, K., Singer, J., "Dynamic yield and tensile strength of aluminum single crystals at temperatures up to the melting point", Journal of Applied Physics **90**, 136, 2001.
6. Chen, X., J.R. Asay, and S.K., Field, D.P. Dwivedi. "Spall behavior of aluminum with varying microstructures." Journal of Applied Physics **99**, 023528, 2006.